Pulsed Electron Beam Initiation in Emulsion Polymerization

Jens Pusch and Alex M. van Herk*

Laboratory of Polymer Chemistry, Eindhoven University of Technology, P.O. Box 513, 5600 MB Eindhoven, The Netherlands

Received January 31, 2005; Revised Manuscript Received July 26, 2005

ABSTRACT: Electron irradiation as an alternative to chemical initiation in emulsion polymerization is a well-known but not widely used technique. Accelerated electrons create the initiating radical species by scission of molecules that are present in the reaction mixture. The initiation mechanism in detail is so far not completely understood due to the broad variety of radical species that are created by the electron beam. The pulsed electron beam polymerization (PEBP) of methyl methacrylate (MMA), ethyl methacrylate (EMA), and butyl methacrylate (BMA) was analyzed with matrix-assisted laser desorption/ionization time-of-flight mass spectrometry (MALDI-TOF MS) to shine light onto the main initiating species of the PEBP but also on the polymer decomposition that occurred under pulsed electron beam irradiation. Hydrogen and hydroxyl radicals were identified as the main initiating species in polymerization of the investigated monomers. An increasing degree of initiation by monomer radicals was observed with decreasing water solubility of the polymerized monomer.

Introduction

Emulsion polymerization today is predominantly initiated by radicals produced through chemical initiation. Although the high-energy radiation (HER) like γ-, ultrasound, and pulsed electron beam (PEB) irradiation have been intensively investigated, they are not commonly used as initiation methods. Early points of interest were, due to a controlled radical flux, possible kinetic differences between this system and chemical initiation. Also, the possibility of initiating polymerizations at low temperatures and the synthesis of latices with small particle sizes are challenges. The initiation with γ- and PEB irradiations, using a Co^{60}-source or accelerated electrons, has been studied by polymerization of a large number of monomers in the laboratory setup, including vinyl acetate (VAc), styrene (Sty), methyl-, butyl-, and dodecyl methacrylates (MMA, BMA, DMA), methyl-, ethyl-, and *n*-butyl acrylates (MA, EA, BA), butadiene, isoprene, and vinyl chloride. Stannett and Stahel have provided an overview of the research done in the field of HER-initiated emulsion polymerization.[1]

A major drawback of HER is the rather complex setup that requires installing a radiation source. Another disadvantage is that irradiation not only creates radicals but also tends to destroy the formed polymer. Furthermore, ionic groups, originating from the chemical initiators that might provide additional latex stability, are lacking in HER.[2] With regard to the financial factor, a cost analysis demonstrated that the monetary investment is similar for both chemically and irradiation-initiated polymerization.[3]

On the other hand, HER has many advantages over chemical initiation which have been shown in this work and previous papers of our group; at this point we feel it is useful to summarize all the advantages.

(1) The first one is the controllable and stable flux of radicals, which is dependent on the irradiation intensity. This makes HER interesting as a tool for mechanistic and kinetic research[4] as has been shown also in a previous paper in this journal [Pusch, J.; van Herk, A. M. *Macromolecules*, in press].

Scheme 1. Important Reactions Occurring during the Radiolysis of Water[8]

$$H_2O + e^- \longrightarrow H^- + {}^\bullet OH \quad (1)$$

$$H_2O + e^- \longrightarrow {}^\bullet H + OH^+ + 2e^- \quad (2)$$

$$H_2O + e^- \longrightarrow H^+ + {}^\bullet OH + 2e^- \quad (3)$$

$$H_2O + e^{-*} \longrightarrow H_2O^* + e_{aq}^- \quad (4)$$

$$H_2O^* \longrightarrow {}^\bullet H + {}^\bullet OH \quad (5)$$

(2) The second advantage is that the radical flux is independent of temperature. Whereas in chemical initiation a certain temperature is necessary for significant decomposition of the initiator, e.g., peroxides, HER creates radicals independent of temperature. This makes HER very interesting for the emulsion polymerization of VAc, a monomer that has a high chain transfer rate, especially at high temperatures. These chain transfer effects lead to low molecular weights, which are not desired in the industrial production of PVAc. The independence of temperature explains why HER is nearly exclusively applied in studies with a pilot plant on VAc, especially at low temperatures.[5−7]

(3) The third advantage of HER as an initiation technique is the type of radicals produced. The PEB irradiation of water results in the formation of various species.

Equations 1−5 in Scheme 1 are a choice of possible reactions occurring in the water phase. Predominantly $OH^\bullet$, $H^\bullet$, e_{aq}^-, and H^+ are created by the radiolysis of water, but also the recombination products H_2O_2 (by recombination of two $OH^\bullet$ radicals) and H_2 (by recombination of two $H^\bullet$ radicals).[8] Hydrogen atoms and especially hydroxyl radicals are neutral and strongly reactive radicals which makes them interesting for radically initiated polymerization. Higher energetic species are marked with an asterisk.

(4) Barriac et al.[2] have pointed out that the ionic strength of the water phase in the HER system is very low because no salts (initiators) are required. In theory,

* Corresponding author: e-mail amvherk@tue.nl.

10.1021/ma050201t CCC: $30.25
Published on Web 09/24/2005

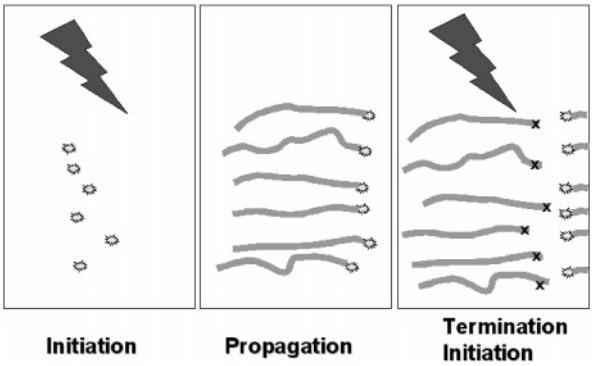

Figure 1. Schematic drawing of pulsed initiated polymerization.[4]

the absence of electrolyte improves the colloidal stability of more and smaller particles. The initiating hydrogen and hydroxyl radicals are also known to diffuse fast.

(5) The pulsed initiation mechanism in HER promotes the formation of polymer chains with low molecular weights. In pulsed electron beam polymerization (PEBP) a constant, large quantity of radicals is created with every pulse, and the radical concentration is much higher than in the steady state of a chemically initiated system. Hence, a large number of particles with polymer chains of fairly low molecular weight will be formed. The mechanism of a pulsed initiated polymerization is shown in Figure 1.

With the first electron beam pulse a burst of radicals is created. Polymerization starts simultaneously with the initiation of many chains that grow continuously. With the next electron beam pulse the majority of these chains is terminated due to the high radical concentration, and only a minority of chains continues to grow, which means that in the final product a majority of polymer chains of identical length, or multiples of that chain length, may be expected. The PEBP experiment has been used as an analytical tool to determine the local monomer concentration in heterogeneous systems.[4] Also, in the previous investigation related to making small latex particles through pulsed electron beam polymerization these fine structures in the GPC tracers have been observed [Pusch, J.; van Herk, A. M. *Macromolecules*, in press]. In contrast to chemically initiated emulsion polymerization, PEBP, with its high radical flux, could create ideal conditions for the synthesis of a high number of smaller and stable latex particles.

Although the PEBP is extensively investigated, the initiation mechanism of the system is so far not completely understood, and assumptions about it are drawn from the radical species present in the emulsion. For a good control of the system and the material properties a better insight into the initiation mechanism is needed. Matrix-assisted laser desorption/ionization time-of-flight mass spectrometry (MALDI-TOF-MS) is a powerful tool for the polymer end-group analysis and allows conclusions from the obtained results as to the initiating species of the polymer chains. The aim of the work described in this paper was to investigate the initiation mechanisms in the PEBP of MMA, EMA, and BMA with MALDI-TOF-MS. A special focus in the investigations was to examine the influence of water solubility of the polymerized monomer on the initiation mechanism. The values for water solubility of the investigated monomers are given in Table 1. The polymerizations were performed at low surfactant concentrations to minimize major initiation by radicalized surfactant molecules.

Table 1. Water Solubility of the Investigated Monomers[8]

monomer	$[M]_{aq}$ (20 °C) (mol L^{-1})
MMA	1.5×10^{-1}
EMA	6.5×10^{-2}
BMA	2.5×10^{-3}

The electron irradiation also leads to polymer decomposition causing difficulties in the analysis of the initiation process. Therefore, the polymer decomposition of an irradiated polymer standard with a defined molecular weight distribution was investigated with MALDI-TOF-MS analysis.

Experimental Section

Characterization. Matrix-assisted laser desorption/ionization time-of-flight mass spectrometry (MALDI-TOF-MS) measurements were made on a Voyager-DE STR (Applied Biosystems, Framingham, MA) instrument equipped with a 337 nm nitrogen laser. Positive-ion spectra were acquired in reflector mode. Dithranol was chosen as the matrix. Potassium trifluoroacetate (Aldrich, 98%) was added as cationic ionization agent. The matrix was dissolved in tetrahydrofuran (THF) at a concentration of 40 mg/mL. Potassium trifluoracetate was added to THF at a concentration of 5 mg/mL. The dissolved polymer concentration in THF was ~1 mg/mL. In a typical MALDI experiment, the matrix, salt, and polymer solutions were premixed in a ratio 5 μL sample:5 μL matrix:0.5 μL salt. Approximately 0.5 μL of the obtained mixture was hand-spotted on the target plate. For each spectrum 1000 laser shots were accumulated.

Molecular weight distributions (MWDs) were measured by SEC at room temperature using a Waters SEC equipped with a Waters model 510 pump and a model 410 differential refractometer (40 °C). THF was used as the eluent at a flow rate of 1.0 mL/min. A set of two linear columns (Mixed-C, Polymer Laboratories, 30 cm, 40 °C) was used. Calibration was carried out using narrow MWD of PSty standards ranging from 600 to 7×10^6 g/mol.

The molecular weights were calculated using the universal calibration principle and Mark−Houwink parameters (PMMA: $K = 9.55 \times 10^{-5}$ dL/g, $a = 0.719$; PSty: $K = 1.14 \times 10^{-4}$ dL/g, $a = 0.716$; PEMA: $K = 9.7 \times 10^{-5}$ dL/g, $a = 0.714$; PBMA: $K = 1.48 \times 10^{-4}$ dL/g, $a = 0.664$; PVAc: $K = 2.24 \times 10^{-4}$ dL/g, $a = 0.674$).[9] Data acquisition and processing were performed using Waters Millennium 32 software.

Materials. The monomers methyl methacrylate (MMA, 99%, Aldrich), ethyl methacrylate (EMA, 99%, Aldrich), and butyl methacrylate (BMA, 99%, Aldrich) were used after being purified from inhibitor by passing them over a column filled with an inhibitor remover package (Aldrich). Sodium dodecyl sulfate (SDS, 96.0%, Fluka) and the polymer standard of PMMA with an M_n of 3437 from Polymer Laboratories were used as received. Deionized water was used in all experiments.

Setup. The Eindhoven Technical University's linear accelerator was used to initiate the polymerization reaction. The accelerated electrons had an energy of 5 MeV. The accelerator is a substantially modified Philips SL 75-5 medical accelerator. Accelerated electrons left the vacuum through a 100 μm aluminum foil scattering the electrons over a mean angle of 8°. The target was placed at a distance of 5 cm from the aluminum foil. The pulse width was 4 μs. The pulse repetition rate was varied between 10, 25, and 50 Hz. Further details can be found in the literature.[10−12]

For the batch reactions a cylindrical, thermostated, double-wall quartz cell of 5 mL volume was used. The inner cell had a diameter of 2.5 cm and a height of 2 cm. A thermostat controlled the temperature of the reactor. After addition of the emulsion the cell was sealed with plastic sealing caps. The cell was fixed in a Lab-Line multiwrist shaker.

PEB Polymerization. In a typical batch polymerization procedure, 4.5 mL of water, 0.5 g of monomer, and 0.015 g of surfactant were emulsified for 5 min on a Whirlimixer. The

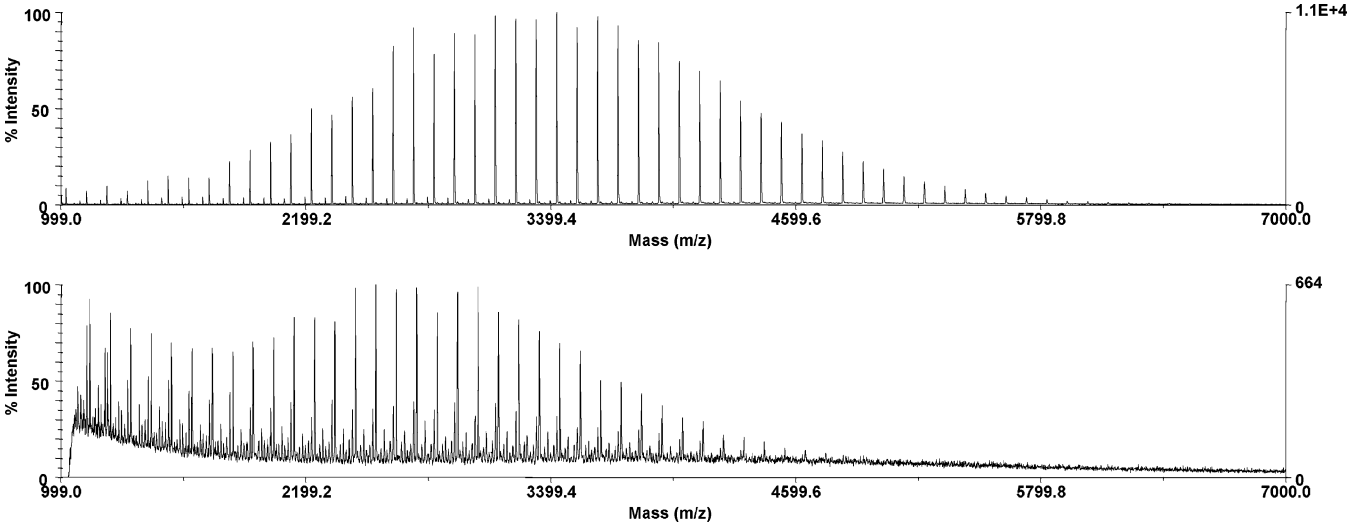

Figure 2. MALDI-TOF MS spectra of standard PMMA with M_n 3437 emulsified in water with 0.3 wt % surfactant before (upper) and after (lower) irradiation with 1140 kGy (10 Hz).

Table 2. SEC Data of the Molecular Weight M_n of a PMMA Standard with an M_n of 3437 Irradiated with Various PEB (10 Hz) Doses

radiation dose (kGy)	M_n
0	3437
380	3194
760	2904
1140	2777

emulsion was then placed in the reaction cell and irradiated at 60 °C with a frequency of 10 Hz.

Results and Discussion

MALDI-TOF MS Analysis of PEB-Induced PMMA Decomposition. One effect of the PEBP is that the irradiation of an emulsion with accelerated electrons not only creates radicals but also tends to destroy the formed polymer. Prior to the analysis of the PEBP initiation mechanism, the irradiation-induced polymer decomposition of PMMA latices MALDI-TOF MS analysis was applied to understand the polymer decomposition. A cationically polymerized PMMA standard (only H end groups) with an M_n of 3437 was emulsified in water, containing 0.3 wt % surfactant, and irradiated with various PEB doses at 10 Hz. The radiation doses and the values obtained for M_n of the PMMA are collected in Table 2.

The results in Table 2 show a decrease in M_n at higher radiation doses. This decrease can be attributed to decomposition of the polymer. Figure 2 shows the MALDI-TOF MS spectra of the PMMA standard before and after being irradiated with a PEB dose of 1140 kGy.

Figure 2 shows the spectra of PMMA with the MMA repeating unit every 100 mass units. As expected, the whole weight distribution is shifted toward lower molecular weights after an applied radiation dose of 1140 kGy, indicating scission of polymer chains.

The decomposition of PMMA under high-energy electron irradiation has been investigated in the past with mass spectroscopy and a residual gas analyzer (RGA).[13−15] Scission of the polymer backbone was the major event observed, but also side-chain scission was detected. The major scission steps for side-chain decomposition are given in Scheme 2 in formulas 6−10 where P stands for polymer backbone. It is possible that a PMMA chain after a side-chain decomposition as mentioned in formulas 6−10 undergoes a second side-chain scission. The probability for a second side-chain scission is somewhat lower but increases with higher radiation doses.

Scheme 2. Major Irradiation-Induced Scission Steps for Side-Chain Decomposition

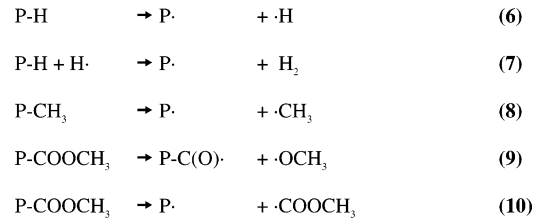

A close-up on the MALDI-TOF MS spectra of a PMMA standard irradiated at low and high radiation doses is given in Figure 3. It confirms the increase in side-chain decomposition at higher radiation doses.

The MALDI-TOF MS samples were prepared with potassium ions. The main polymer chain without any side-chain damage is represented by the peaks at 2243 and 2343 Da. These peaks can be attributed to the molecules $[H\text{-}(MMA)_{22}H]K^+$ and $[H\text{-}(MMA)_{23}H]K^+$. The upper spectrum of Figure 3 shows that after a low radiation dose three side-chain scission peaks can be detected at 2329, 2313, and 2283 Da. These peaks arise from primary side-chain damage; the decomposition mechanisms are given in the schemes 8−10. At higher radiation doses (lower spectrum) two more peaks arise at 2268 and 2312 Da. These peaks can be attributed to polymeric chains undergoing two side-chain break events. This secondary decomposition is expected to be predominantly the loss of a CH_3 group at "the other end" of the polymer backbone.

The assignment of the fragmentation peaks seen in MALDI-TOF MS is given in Table 3. Once a polymeric chain has fragmented into radicals, these radicals undergo further reactions like recombination or (most likely) hydrogen abstraction, which further complicates the interpretation of the spectra. Not all peaks were therefore assigned in the same detailed way as the main polymer chain peaks.

MALDI-TOF MS Analysis of PEB-Initiated PMMA Latex. The MALDI-TOF MS spectrum of PEBP PMMA shows a homogeneous repeating pattern (Figure 4). The

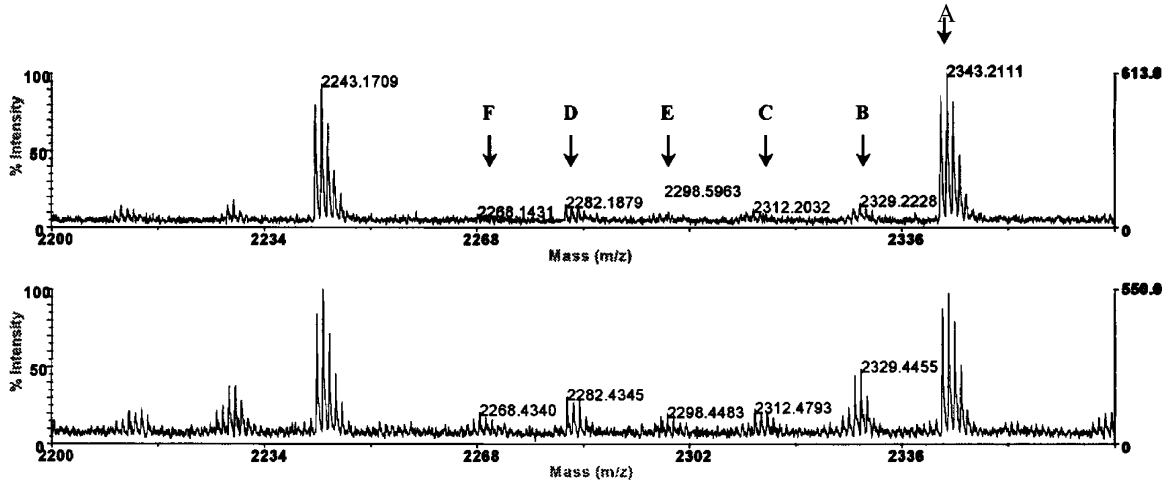

Figure 3. MALDI-TOF MS spectra of PMMA standard with M_n 3437 emulsified in water with 0.3 wt % surfactant, irradiated at 380 kGy (10 Hz) (upper) and 1140 kGy (10 Hz) (lower). Peak A represents $[H\text{-}(MMA)_{23}H]K^+$, and peaks B−F are fragmentation peaks of peak A which are assigned in Table 3.

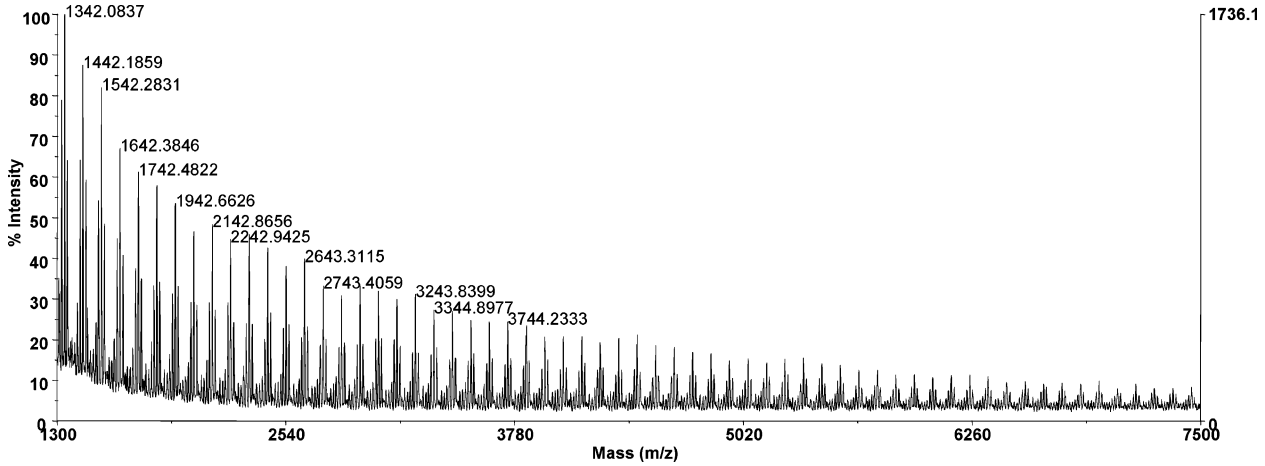

Figure 4. MALDI-TOF MS spectrum of PMMA latex produced with PEB initiated emulsion polymerization of MMA emulsified with 0.3 wt % SDS irradiated with 380 kGy (10 Hz).

Table 3. Fragmentation Peaks and the Accompanying Decomposition Schemes of the MALDI-TOF MS Spectra (Figure 3) of a PMMA Standard Emulsified in Water, Irradiated with PEB (10 Hz)

peak (Figure 3)	peak (Da)	fragmentation	decomposition formula (Scheme 2)
A	2343	$[H\text{-}(MMA)_{23}H]K^+ = PK^+$	
B	2329	$[P\text{-}CH_3]K^+ \rightarrow [P_B^{\bullet}]K^+ + {}^{\bullet}CH_3$	8
C	2313	$[P\text{-}COOCH_3]K^+ \rightarrow [P_C\text{-}C(O)^{\bullet}]K^+ + {}^{\bullet}OCH_3$	9
E	2298	peak C $\rightarrow [P_E^{\bullet}]K^+ + {}^{\bullet}CH_3$	9 and 8
D	2283	$[P\text{-}COOCH_3]K^+ \rightarrow [P_D^{\bullet}]K^+ + {}^{\bullet}COOCH_3$	10
F	2268	peak D $\rightarrow [P_F^{\bullet}]K^+ + {}^{\bullet}CH_3$	10 and 9

pattern has a repeating unit of exactly 100, the mass of one MMA unit.

The measured isotopic pattern of the main polymer peak $[H\text{-}(MMA)_{23}H]K^+$, a close-up of Figure 4, corresponds with the calculated pattern (Figure 5).

Figure 6 compares the close-up of the spectra of Figure 4, PMMA latex produced by PEB initiation, with the irradiated PMMA standard of Figure 3.

The comparison of the MALDI-TOF MS spectrum of the PEB irradiated PMMA standard (Figure 3), which was not polymerized with PEB initiation, with the PEB initiated PMMA shows similar peaks of the main polymeric chains and the decomposition products. In addition to the expected peaks, in the lower spectrum of Figure 6 a peak appears, labeled G, 16 Da ahead of the main polymer peak. This peak can be assigned to $HO\text{-}(MMA)_{23}H$.

The peak of $HO\text{-}(MMA)_{23}H$ cannot be observed in the spectrum of the irradiated PMMA standard, and one can therefore exclude that $HO\text{-}(MMA)_n\text{-}H$ originates from a possible recombination of a polymeric radical with an OH radical. This peak can rather be attributed to initiation by OH radicals in the PEBP of the MMA. This provides evidence that H radicals (peak A) and OH radicals (peak G) initiated the PEBP of MMA. Proof for initiating species created by the radiolysis of surfactant was not found. The other peaks in the MALDI-TOF MS spectra of the PEBP of MMA could be attributed to chain decomposition products.

PEB-Initiated Emulsion Polymerization of EMA. Ethyl methacrylate (EMA) has a similar chemical structure as MMA, but because of the additional methylene group it is less water-soluble (see Table 1). EMA was polymerized at low surfactant concentrations with

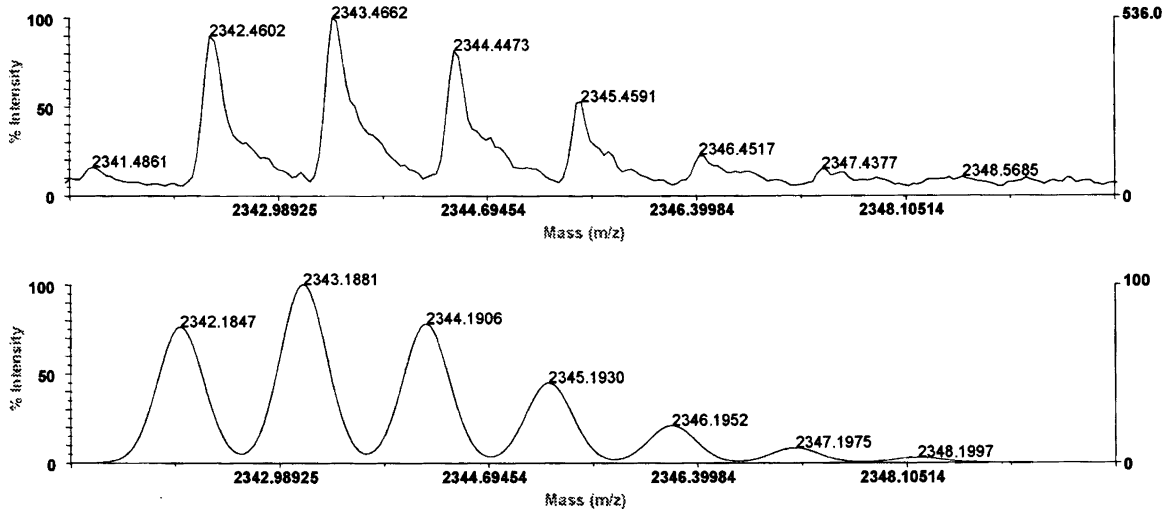

Figure 5. Measured (upper, detail of Figure 4) vs calculated (lower) MALDI-TOF MS isotopic spectra of PEBP [H-(MMA)$_{23}$H]-K^+.

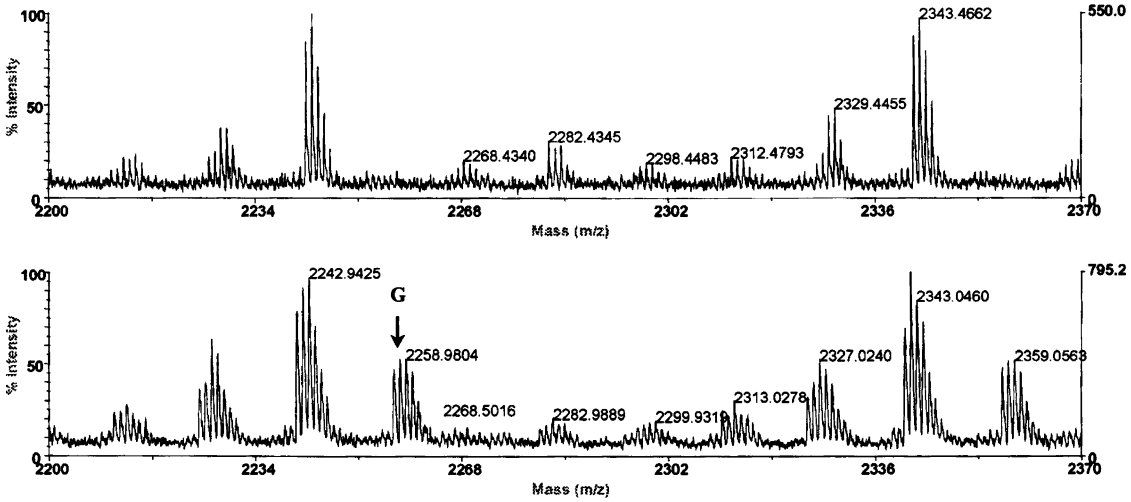

Figure 6. MALDI-TOF MS spectrum of standard PMMA with an M_n of 3437 irradiated with 1140 kGy (10 Hz) (upper, see also Figure 3) vs the spectrum of PMMA latex produced by PEB initiation (below, detail of Figure 4) emulsified with 0.3 wt % surfactant, irradiated with 380 kGy (10 Hz).

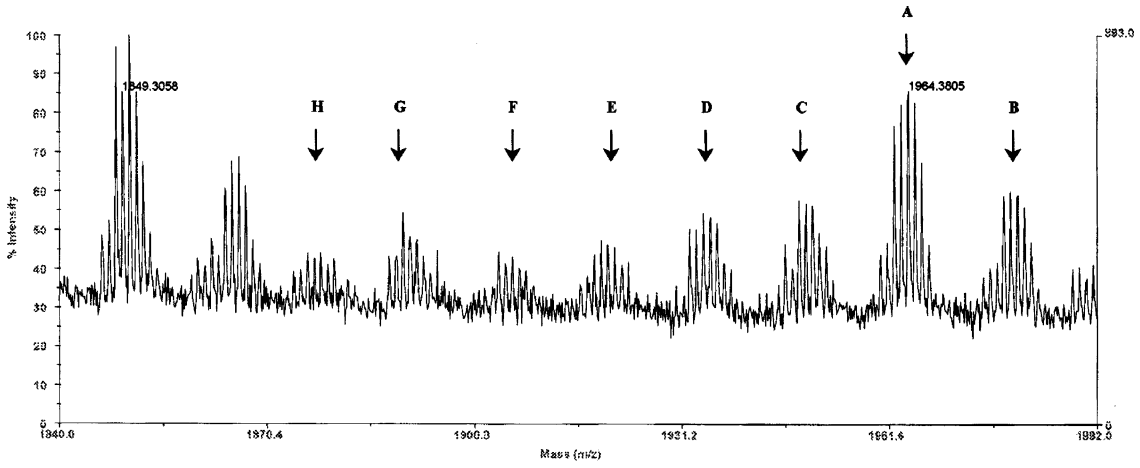

Figure 7. MALDI-TOF MS spectrum of PEMA latex produced by PEB initiated emulsion polymerization of EMA polymerized with 0.3 wt % SDS and irradiated with 380 kGy (10 Hz). The A−H are assigned in Table 4.

PEB initiation to investigate the effect of water solubility of the polymerized monomer on the PEBP.

Figure 7 shows the fragmentation spectrum of PEMA between two repeating units. Similar to PMMA, a peak for a hydroxyl functional polymer chain (peak H) indicates that also hydroxyl radicals initiated EMA. The decomposition of PEMA due to PEB irradiation is analogous to the PMMA fragmentation, except that PEMA has one more methylene group in the side chain resulting in a more complex fragmentation pattern. The comparison between the measured and calculated MALDI-TOF MS isotopic spectra of [H-(EMA)$_{17}$H]K^+ exhibits

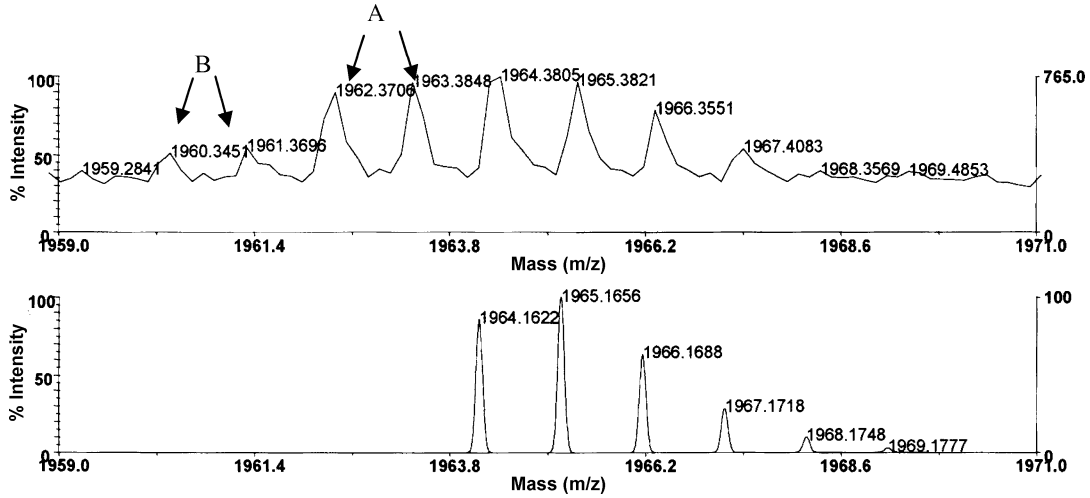

Figure 8. Measured (upper, detail of Figure 7) vs calculated (lower) MALDI-TOF-MS isotopic spectrum spectra of $[H\text{-}(EMA)_{17}\text{-}H]K^+$, of a PEBP PEMA latex.

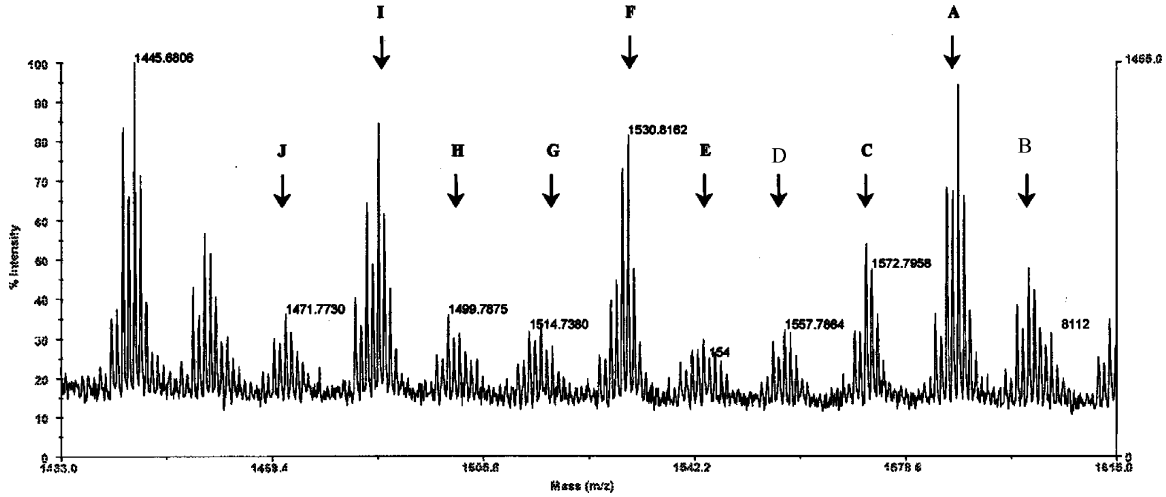

Figure 9. MALDI-TOF MS spectrum of a PEB initiated PBMA latex emulsified with 0.3 wt % surfactant irradiated with 380 kGy (10 Hz). Peaks A−J are assigned in Table 5.

a distinction. Figure 8 depicts more peaks in the measured spectrum than in the calculated pattern. This effect can be explained by the polymerization initiation by monomer radicals, which still had a double bond. Because of the poor water solubility of EMA, the initiation in micelles, particles, and monomer droplets with monomer radicals plays a more important role than in the case of the better water-soluble MMA, resulting in a peak 2 Da lower (peak A). The small peak 4 Da below the calculated pattern (peak B) is obviously due to disproportionation of the polymeric chains initiated with monomer radicals shifting the pattern once more 2 Da lower.

PEB-Initiated Emulsion Polymerization of BMA. The PEBP of butyl methacrylate (BMA) confirms the effect of the water solubility of the polymerized monomer in PEBP as seen before with MMA and EMA. Because of its butyl group, BMA is less water-soluble than MMA and EMA (see Table 1).

Figure 9 depicts the fragmentation spectrum of the PBMA between two repeating units. Similar to PMMA and PEMA, the peak for the hydroxyl functional oligomer (peak J) indicates that hydroxyl radicals also initiated the polymerization of BMA. The fragmentation of the PBMA due to PEB irradiation is again similar to the PMMA and PEMA decomposition. Extra methylene groups in the side chain make the fragmentation pattern more complex than for MMA and EMA. The comparison between the measured and calculated MALDI-TOF MS isotopic spectra of $[H\text{-}(BMA)_{11}H]K^+$ in Figure 10 showed the same effects as seen with EMA. The high extent of the initiation by monomer radicals, which still had a double bond, resulted in peaks 2 Da below the main molecular peak (peak A). The small peak 4 Da below the calculated pattern (peak B) is again due to disproportionation of the polymeric chains initiated with monomer radicals.

Table 4. Fragmentation Peaks of the MALDI-TOF MS Spectra (Figure 7) of PEMA Latex Polymerized with 0.3 wt % SDS and Irradiated with 380 kGy (10 Hz)

peak (Figure 7)	peak (Da)	fragmentation
B	1980	$[H\text{-}(EMA)_{17}OH]\ K^+ = [P\text{-}OH]K^+$
A	1963	$[H\text{-}(EMA)_{17}H]K^+ = PK^+$
C	1948	$[P\text{-}CH_3]K^+ \rightarrow [P_C{\bullet}]K^+ + {\bullet}CH_3$
D	1934	$[P\text{-}C_2H_5]K^+ \rightarrow [P_D{\bullet}]K^+ + {\bullet}C_2H_5$
E	1918	$[P\text{-}COOC_2H_5]K^+ \rightarrow [P_E\text{-}C(O){\bullet}]K^+ + {\bullet}OC_2H_5$
F	1903	peak E $\rightarrow [P_F{\bullet}]K^+ + {\bullet}CH_3$
G	1890	$[P\text{-}COOC_2H_5]K^+ \rightarrow [P_G{\bullet}]K^+ + {\bullet}COOC_2H_5$
H	1875	peak G $\rightarrow [P_H{\bullet}]K^+ + {\bullet}CH_3$

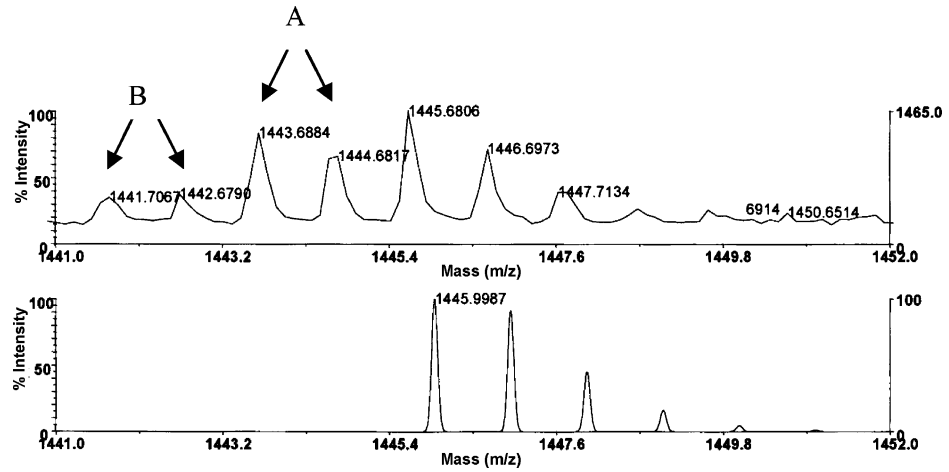

Figure 10. Measured (upper, detail of Figure 9) vs calculated (lower) MALDI-TOF-MS isotopic spectra of $[H\text{-}(BMA)_{11}H]K^+$, of a PEB-initiated PBMA latex.

Table 5. Fragmentation Peaks of the MALDI-TOF MS Spectra (Figure 9) of a PEB-Initiated PBMA Latex Emulsified with 0.3 wt % Surfactant Irradiated with 380 kGy (10 Hz)

peak (Figure 9)	peak (Da)	fragmentation
B	1603	$[H\text{-}(BMA)_{11}OH]K^+ = [P\text{-}OH]K^+$
A	1587	$[H\text{-}(BMA)_{11}H]K^+ = PK^+$
C	1572	$[P\text{-}CH_3]K^+ \rightarrow [P_C^{\bullet}]K^+ + {}^{\bullet}CH_3$
D	1558	$[P\text{-}C_2H_5]K^+ \rightarrow [P_D^{\bullet}]K^+ + {}^{\bullet}C_2H_5$
E	1544	$[P\text{-}C_3H_7]K^+ \rightarrow [P_E^{\bullet}]K^+ + {}^{\bullet}C_3H_7$
F	1530	$[P\text{-}C_4H_9]K^+ \rightarrow [P_F^{\bullet}]K^+ + {}^{\bullet}C_4H_9$
G	1514	$[P\text{-}COOC_2H_5]K^+ \rightarrow [P_G\text{-}C(O)^{\bullet}]K^+ + {}^{\bullet}OC_4H_9$
H	1499	peak G $\rightarrow [P_H^{\bullet}]K^+ + {}^{\bullet}CH_3$
I	1486	$[P\text{-}COOC_4H_9]K^+ \rightarrow [P_I^{\bullet}]K^+ + {}^{\bullet}COOC_4H_9$
J	1471	peak I $\rightarrow [P_J^{\bullet}]K^+ + {}^{\bullet}CH_3$

Conclusions

The electron irradiation as an alternative to chemical initiation in emulsion polymerization was investigated with focus on the initiation mechanism and polymer decomposition occurring in the system. The MALDI-TOF MS analysis of cationically polymerized poly(methyl methacrylate) (PMMA) standards emulsified in water and irradiated with accelerated electrons showed decomposition of the polymer by scission in the main chain but also the side chain.

Matrix-assisted laser desorption/ionization time-of-flight mass spectrometry (MALDI-TOF MS) analysis of latices initiated by pulsed electron beam polymerization (PEBP) of methyl methacrylate (MMA), ethyl methacrylate (EMA), and butyl methacrylate (BMA) identified hydrogen and hydroxyl radicals as the main initiating species of the PEBP. An increasing degree of initiation by monomer radicals was observed with decreasing water solubility of the polymerized monomer. The polymer decomposition that occurred under pulsed electron beam (PEB) irradiation and the major irradiation decomposed polymeric species were also identified within the performed investigations.

References and Notes

(1) Stahel, E. P.; Stannett, V. T. In *Large Radiation Sources for Industrial Processes*; International Atomic Energy Agency: Vienna, 1969.
(2) Barriac, J.; Oda, E.; Russo, S.; Knorr, R.; Stahel, E. P.; Stannet, V. *ACS Adv. Chem. Ser.* **1976**, *24*, 142.
(3) Allen, R. S.; Ransohoff, J. A.; Woodard, D. G. *Isot. Radiat. Technol.* **1971**, 992.
(4) van Herk, A. M.; de Brouwer, H.; Manders, B. G.; Luthjens, L. H.; Hom, M. L.; Hummel, A. *Macromolecules* **1996**, *29*, 102.
(5) Singh, A.; Silverman, J. *Radiation Processing of Polymers;* Oxford University Press: New York, 1992; p 289.
(6) Allen, R. S.; Ransohoff, J. A.; Woodard, D. G. U.S. Atomic Energy Agency Report TID-4500 (Oro-673), 1969.
(7) O'Neill, T.; Pinkava, J.; Hoigne, J. In *Proceedings of the Third Tihany Symposium on Radiation Chemistry*; Dobo, J., Hedvig, P., Schiller, R., Eds.; Akademiai kiado: Budapest, 1972; Vol. 1.
(8) *Course on Emulsion Polymerisation*, Script; SEP: Eindhoven, 2001.
(9) Beuermann, S.; Paquet, D. A., Jr.; McMinn, J. H.; Hutchinson, R. A. *Macromolecules* **1996**, *29*, 4206.
(10) Botman, J. I. M.; Derksen, A. T. A. M.; van Herk, A. M.; Jung, M.; Kuchta, F.-D.; Manders, L. G.; Timmermans, C. J.; de Voigt, M. J. *Nucl. Instrum. Methods Phys. Res., Sect. B* **1998**, *B139*, 1−4, 490.
(11) Van Duijneveldt, W.; Botman, J. I. M.; Timmermans, C. J.; De Leeuw, R. W. *Nucl. Instrum. Methods Phys. Res., Sect. B* **1993**, *B79*, 871.
(12) Derksen, A. T. A. M.; Timmermans, C. J.; Wintraeken, Y. J. E.; Botman, J. I. M.; Fiedler, H.; Hagedoorn, H. L. *Proc. 5th Eur. Particle Accelerator Conf. Barcelona, Spain* **1996**, 2699.
(13) Todd, A. *J. Polym. Sci.* **1960**, *42*, 223.
(14) Venkatesan, T.; Edelson, D.; Brown, W. L. *Appl. Phys. Lett.* **1983**, *43*, 4, 364.
(15) Lee, E. H.; Rao, G. R.; Mansur, L. K. *Radiat. Phys. Chem.* **1999**, *55*, 293.

MA050201T